

Atomic-scale imperfections and fluctuations in the transmission properties of a quantum dot

S. K. Kirby, D. Z.-Y. Ting, and T. C. McGill

Thomas J. Watson, Sr., Laboratory of Applied Physics, California Institute of Technology, Pasadena, California 91125

(Received 4 April 1994; revised manuscript received 14 July 1994)

We examine the effects of atomic-scale imperfections on the transmission properties of a quantum dot resonant tunneling structure. For this purpose, we employ a three-dimensional model of quantum transport. We find that variation in the surface roughness of quantum dots leads to substantial fluctuations in the transmission properties. Impurities in a quantum dot are studied as a function of impurity strength and location, and it is found that an attractive impurity near the center of a dot can reduce fluctuations caused by surface roughness. Nevertheless, the presence of more than a single impurity can give rise to a complex resonance structure that varies substantially with impurity configuration.

I. INTRODUCTION

State-of-the-art fabrication techniques such as molecular beam epitaxy and nanolithography have given rise to a new generation of mesoscopic structures such as double barrier resonant tunneling diodes, quantum wires, and quantum dots. These structures hold promise as the basis of a new technology for building smaller devices with new functionality, yet they also present new challenges. With characteristic dimensions comparable to the electron deBroglie wavelength, these structures operate in the quantum regime and they are particularly sensitive to atomic-scale variations in geometry and composition. Defect impurities and interface roughness, for example, can dramatically alter the properties of a quantum device. In this paper we focus on fluctuations in the transmission properties of a quantum dot resonant tunneling structure due to compositional and structural variations.

Quantum dots and quantum wire-shaped electron waveguides have been produced by a variety of techniques.¹⁻⁸ On account of their small dimensions quantum wires are very difficult to fabricate, and most quantum wires exhibit structural variation. Interface roughness over the scale of a few monolayers is currently unavoidable in etched quantum wires. In addition, compositional variation, particularly due to impurities, is difficult to eliminate. As a consequence, the effects of these variations on device performance have drawn considerable attention.

Theoretical studies of interface roughness in quantum wires have revealed alterations of the transmission spectra. A small width increase in one place in a quantum wire has been shown to produce dips in the well-known steplike conductance structure.⁹ It has also been shown that cross-sectional area variations along a wire lead to a smearing of the peaklike structure of the average density of states plotted as a function of carrier energy.¹⁰

Impurities in quantum wires have been studied both experimentally and theoretically. An isolated conductance peak observed below the turn-on of the first trans-

verse mode in a narrow constriction has been attributed to resonant tunneling via a single impurity.¹¹ Degradation in the quantized conductance steps of a dual electron waveguide has been seen when the conductance channel is electrostatically steered into a scatterer.¹² Theoretical studies of an impurity in a narrow channel have revealed the ways in which scattering from the impurity alters the transmission properties.¹³⁻¹⁵ In these papers, dips, peaks, and shifts in the conductance and transmission coefficient curves as a function of impurity location and strength have been calculated. Calculations involving a T-shaped quantum wire junction have shown that a repulsive impurity can either enhance or suppress transmission.¹⁶ Impurities near the aperture of a waveguide have been shown to destroy quantized conductance¹⁷ and ionized donors have been shown to affect the quantized conductance of point contacts in a way that reflects the detailed configuration of the impurities.¹⁸

Other investigations of imperfections have been carried out, mostly by way of specific examples. If quantum devices are to become commercially viable as components of mass-produced circuits, however, statistical fluctuations in imperfections from device to device must be considered. In this paper we address fluctuations in the transmission spectrum due to variations in interface roughness and impurities in a quantum dot resonant tunneling structure. For this purpose we have developed a supercell model of quantum transport capable of representing variation in three dimensions. This allows us to study novel geometries such as quantum wires and dots with structural and compositional variations.

An outline of the paper is as follows. In Sec. II we describe the supercell method and how it can be used to simulate low-dimensional structures. In Sec. III we apply the method to quantum dots with interface roughness and impurities. We first examine fluctuations in the transmission resonance position and width with different interface roughness configurations of the same statistical description. We then study the influence of impurity

strength and location on the transmission resonances of a quantum dot with interface roughness. We summarize and conclude in Sec. IV.

II. METHOD

Our supercell model of quantum transport is based on the one-band, nearest neighbor, cubic lattice tight-binding Hamiltonian

$$H = \sum_{\mathbf{n}} \epsilon_{\mathbf{n}} |\mathbf{n}\rangle \langle \mathbf{n}| + \sum_{\langle \mathbf{n}\mathbf{m} \rangle} t_{\mathbf{n}\mathbf{m}} |\mathbf{n}\rangle \langle \mathbf{m}|, \quad (1)$$

where the second sum extends over all nearest neighbor pairs on a cubic lattice of lattice constant a . Each of the sites \mathbf{n} is associated with two material parameters: a band edge $E_{\mathbf{n}}$ and an effective mass $m_{\mathbf{n}}$. In terms of these parameters, the on-site energies $\epsilon_{\mathbf{n}}$ and the hopping matrix elements $t_{\mathbf{n}\mathbf{m}}$ used in the Hamiltonian are, following Frensley,¹⁹

$$\begin{aligned} \epsilon_{\mathbf{n}} &= E_{\mathbf{n}} - \sum_{\mathbf{m}} t_{\mathbf{n}\mathbf{m}}, \\ t_{\mathbf{n}\mathbf{m}} &= \frac{1}{2}(t_{\mathbf{n}} + t_{\mathbf{m}}), \\ t_{\mathbf{n}} &= -\frac{\hbar^2}{2m_{\mathbf{n}}a^2}. \end{aligned} \quad (2)$$

The sum in the first line above is over all nearest neighbor sites \mathbf{m} of site \mathbf{n} . These definitions are familiar when one considers the special case of a uniform bulk material of band edge E_0 and effective mass m in which case the Hamiltonian gives rise to the band structure

$$E(\mathbf{k}) = E_0 - 2t(3 - \cos k_x a - \cos k_y a - \cos k_z a), \quad (3)$$

where $t = -\hbar^2/2ma^2$.

In order to make transport calculations numerically tractable, we apply a planar supercell method to this Hamiltonian. We model a three-dimensional device structure as a series of monolayer planes along the z direction. Each plane consists of an infinite periodic array of identical rectangular supercells n_x sites in the x direction and n_y sites in the y direction, as in Fig. 1. The sites for the supercell in a particular plane are chosen to reflect the properties of that plane. For example, if the plane represents a region of bulk material, the sites are identical. To represent a cross-sectional plane of a quantum dot with interface roughness and an impurity in the plane we configure the supercell as in Fig. 1. Three materials are represented: one for the impurity and one each for the interior of the dot and the confining region, which meet at a rough interface. Thus in the supercell method, the infinite layers normal to the growth direction are modeled by a finite supercell, and a device structure is specified by a finite series of supercells along the growth direction.

To calculate quantum transport in this model, we use an efficient, numerically stable method.^{20–22} The transmission coefficients for structures described by the super-

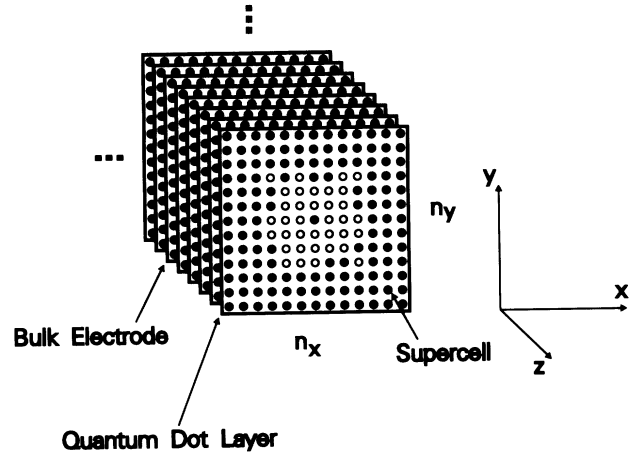


FIG. 1. Supercell representation of a quantum dot resonant tunneling structure with rough walls and an impurity in the cavity. The supercells repeat in the planes normal to the z direction.

cell model can be determined by the direct application of the multiband method described by Ting *et al.*²² The Hamiltonian matrix elements, together with terms representing the boundary conditions in the electrodes, enter into a linear system of equations, which is solved for the electron wave function using an iterative algorithm.^{23,24} From this the transmission can be determined.²²

III. RESULTS AND DISCUSSION

A. Interface roughness fluctuations

Our first application of the supercell model is to study the effects of interface roughness fluctuations in quantum dot resonant tunneling structures. The quantum dots we shall study consist of a cavity surrounded by confining walls and sandwiched between two electrodes along the z direction. The center of the dots is taken as $x = y = z = 0$. The confining walls are made of barrier material, characterized by a band edge of $E_b = 1.05$ eV and an effective mass of $m_b = 0.1248m_0$, the cavity is composed of well material with a band edge of $E_w = 0$ eV and an effective mass of $m_w = 0.0673m_0$, and the electrodes have a band edge of $E_e = -1$ eV and an effective mass of $m_e = 0.1m_0$. These material parameters were chosen so that the well material corresponds to GaAs, and the barrier material corresponds to AlAs. The electrode band edge is chosen below that of the well to permit study of strongly attractive impurities, giving rise to resonances below the well band edge. A 13×13 supercell is used with a cubic lattice constant of $a = 0.5$ nm.

In Fig. 2 we plot transmission coefficients for a set of ten quantum dots with interface roughness. The transmission coefficients are calculated for plane waves incident along the z direction with no momentum in the x or y directions. The cavity in these dots measures $2.5 \times 2.5 \times 3.5$ nm and is surrounded by a 0.5 nm thick rough interface which is a mixture of approximately 50%

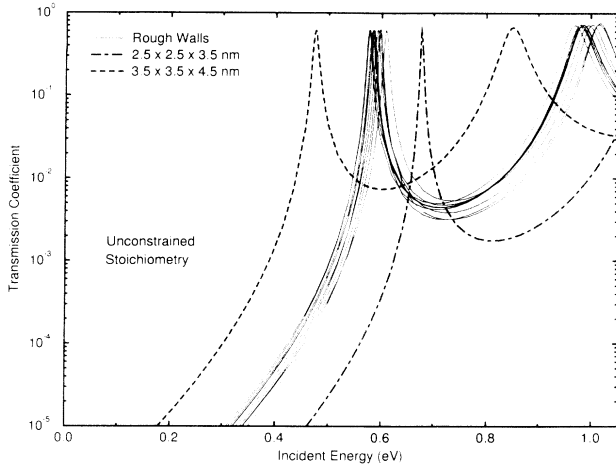


FIG. 2. Transmission coefficient curves for quantum dots with ten different rough-walled configurations. Transmission coefficient curves for two reference smooth-walled dots whose dimensions represent the range of dimensions of the rough-walled dots are also shown. $a = 0.5$ nm, 13×13 supercell, $E_e = -1$ eV, $m_e = 0.1m_0$, $E_b = 1.05$ eV, $m_b = 0.1248m_0$, $E_w = 0$ eV, and $m_w = 0.0673m_0$. Plane waves are incident along the z direction.

well material and 50% barrier material. The shell is constructed one site at a time, each site having a probability 0.5 of being well type and 0.5 of being barrier type, without correlation. Also plotted in the figure for reference are transmission coefficient curves for two ideal dots with smooth walls, whose dimensions represent the range of dimensions of the dots with rough walls. Two layers of barrier material separate the dots from the electrodes on each end.

We see immediately that the resonance position varies over a range comparable to the resonance width. In fact the standard deviation of the $n = 1$ resonance position $[\langle (E_1 - \langle E_1 \rangle)^2 \rangle]^{1/2}$, is about 0.008 eV for the ten samples in Fig. 2, whereas the average intrinsic resonance width ΔE_1 is about 0.009 eV. Since the dots with interface roughness are, in some sense, structural interpolations between the two reference structures, we might expect their resonance widths to fluctuate between the widths of these structures. We found this to be the case, and the standard deviation of the resonance widths of the structures with interface roughness is 11% of the difference between the widths of the two reference structures.

These fluctuations can be attributed to two sources in the rough interface surrounding the quantum dot: fluctuations in stoichiometry and variations in the configuration. Stoichiometric variation arises from the method used to generate the rough interfaces in Fig. 2: each site in the shell of roughness is chosen with a probability 0.5 of being well material and a probability 0.5 of being barrier material. The shells of interface roughness for the ten samples in Fig. 2 are therefore composed of a fraction x of well material and a fraction $1 - x$ of barrier material, where the standard deviation σ_x is about 0.04 and the

average of x is about 0.50. Thus, as the total number of well-type sites in the shell varies, thereby changing the effective sizes of the quantum dots, different confinement energies are produced. We can separate this variation from that of the configuration by constraining the stoichiometry in the shell. We plot in Fig. 3 transmission coefficient curves for a set of ten rough-walled dots with stoichiometry constrained so that the total number of barrier sites in the shell is 134 (out of 266 total sites). Each dot thus contains the same amount of well material (i.e., $\sigma_x = 0$), but a different roughness configuration. The transmission properties still fluctuate, but not as much as with the unconstrained stoichiometry structures ($\sigma_x = 0.04$). In this case, the standard deviation of the resonance widths for the ten samples is 5% of the difference between the widths of the two reference structures.

These fluctuations can be understood on the basis of an analysis of the electron wave function at the resonance. We first calculate the total electron probability density in the quantum dot structure, including all sites in the supercells containing barrier material. We then calculate the total electron probability density in the 0.5 nm shell of interface roughness and express this as a percentage of the total. At the $n = 1$ resonance in a dot with interface roughness, about 27.2% of the total electron probability density lies in the shell containing the roughness. Thus electrons sample the roughness substantially and variations in the roughness configuration can be expected to have a significant impact. This suggests that, if the resonance mode could be altered so as to draw the resonance wave function away from the roughness, fluctuations might be reduced. As a thought experiment, we could place an attractive impurity in a quantum dot, drawing the wave function in toward the impurity site. In the next section we analyze impurities in a dot with rough walls in order to determine what impurity strength should be used and where the impurity should be located to achieve this.

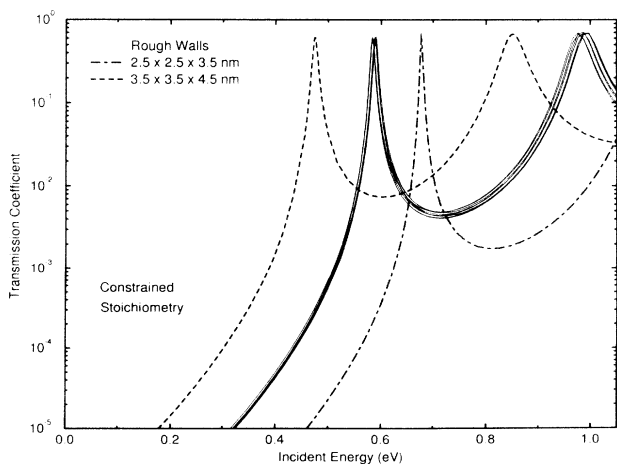


FIG. 3. Same as Fig. 2, except that the stoichiometry in the shell of roughness is identical in the ten samples.

B. Neutral impurities

We represent an impurity in the supercell model by a single site whose onsite energy is ΔU below that of the surrounding sites. The hopping matrix element to the site t is the same as that in the surrounding material. ΔU is thus positive for an attractive impurity and negative for a repulsive impurity. We shall use the dimensionless quantity $\Delta U/t$ as a measure of impurity strength.

We have calculated a series of transmission coefficient curves for a dot with interface roughness and an impurity in the center. The rough-walled dot is that of sample 1 in Sec. III A and the impurity strength is varied from $\Delta U/t = -4.9$ (strongly attractive) to 2.2 (repulsive). The position (E_1), width (ΔE_1), and transmission maximum of the $n = 1$ resonance are plotted in Fig. 4. We note that for the range of impurity strengths under consideration, repulsive impurities have little effect on the transmission characteristics of the dot and attractive impurities have little effect above $\Delta U/t \approx -3$. In fact, we can divide the plots into two regimes, one where the $n = 1$ resonance has more of the character of the cavity mode of the dot (above about -4.3) and one where

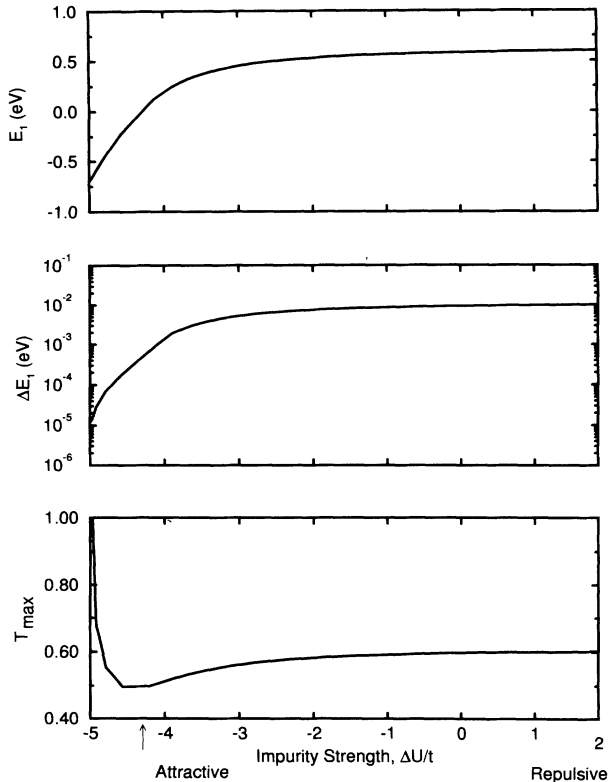


FIG. 4. Characteristics of the $n = 1$ transmission resonance as a function of impurity strength $\Delta U/t$ for a rough-walled dot with a neutral impurity in the center. The rough-walled dot is that of sample 1 in Fig. 2. $a = 0.5$ nm, 13×13 supercell, $E_e = -1$ eV, $m_e = 0.1m_0$, $E_b = 1.05$ eV, $m_b = 0.1248m_0$, $E_w = 0$ eV, and $m_w = 0.0673m_0$. Plane waves are incident along the z direction. The arrow indicates the impurity strength for which the resonance position is at the well material band edge.

it has more of the character of an impurity-bound resonance (below about -4.3). This division makes sense on the basis of an analysis of the resonant wave function: the wave function is similar to that for a dot without an impurity above $\Delta U/t \approx -4.3$ and similar to that for the quasibound state of an attractive impurity²⁵ below -4.3 . In the cavity mode regime ($\Delta U/t > -4.3$), the $n = 1$ resonance is above the well material band edge and the resonance wave function has a standing wave nature in the dot; in the impurity mode regime ($\Delta U/t < -4.3$), the $n = 1$ resonance is below the well material band edge and the resonance wave function decays exponentially with distance from the impurity site. The separation between these two regimes is particularly striking in the bottom panel of Fig. 4, where the maximum transmission coefficient is plotted as a function of impurity strength. In the cavity mode regime, the maximum transmission decreases as the impurity attractive strength increases. In this regime, the impurity perturbs the cavity mode, drawing the resonant wave function in and away from the electrodes, reducing overlap with the electrodes and thus decreasing total transmission. As the impurity strength is further increased, the resonance moves below the well material band edge, into the impurity mode regime. In the case of a very strongly attractive impurity ($\Delta U/t < -5$), the nature of the resonance is almost entirely determined by the impurity. This case is similar to the highly symmetric case of an impurity in the middle layer of a single barrier structure²⁵ and the maximum transmission approaches unity. Thus as impurity strength is increased from the cavity mode regime into the impurity mode regime, the maximum transmission first decreases and then increases to unity, exhibiting a minimum around the point where the resonance position crosses the well material band edge. In the top two panels, we see that the resonance moves toward lower energy and sharpens as the impurity attractive strength is increased below $\Delta U/t = -4$ on account of the increasing localization and confinement of the impurity bound state. Thus choosing $\Delta U/t < -4$ should have a substantial effect in terms of reducing fluctuations due to interface roughness in the cavity.

We next examine impurity location. We analyze the two impurity strength regimes separately, as they give rise to qualitatively different relationships between impurity location and resonance character. Weakly attractive impurities $0 > \Delta U/t > -4.3$ can be analyzed as perturbations to the cavity modes, whereas strongly attractive impurities $\Delta U/t < -4.3$ in a dot behave more like impurities in a single barrier structure.²⁵

In Fig. 5 we plot the $n = 1$ transmission resonance position, width, and maximum for a weakly attractive ($\Delta U/t \approx -3.1$) impurity for different values of the impurity location along the z direction, keeping $x = y = 0$. The $n = 1$ resonance level is lowered more by the attractive impurity potential when the impurity is in the center of the dot than when it is off center, as the $n = 1$ cavity mode has greater probability density in the center and hence samples an impurity more in this position. The maximum transmission increases and the resonance narrows as the impurity perturbs the $n = 1$ mode more to-

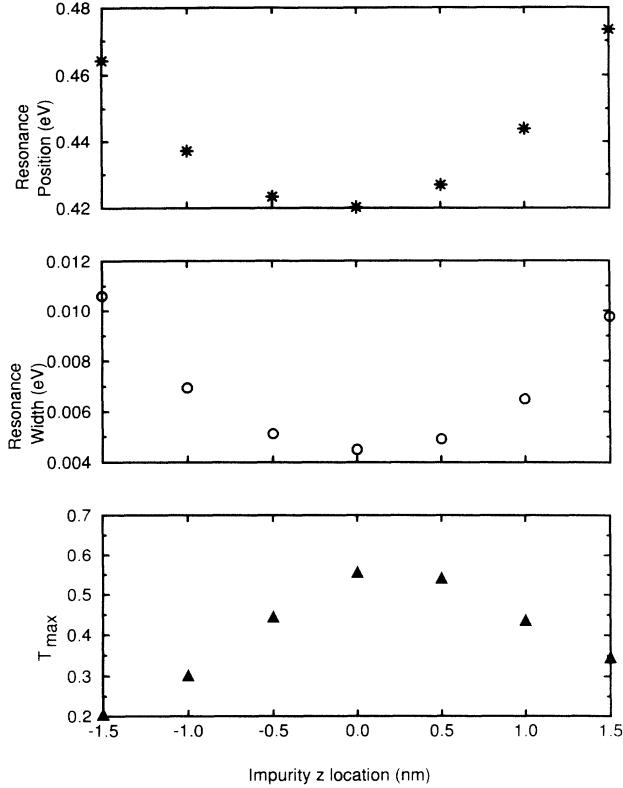


FIG. 5. Characteristics of the $n = 1$ transmission resonance for a rough-walled dot with a weakly attractive impurity ($\Delta U/t \approx -3.1$) in different z locations at $x = y = 0$. The rough-walled dot is that of sample 1 in Fig. 2. $a = 0.5$ nm, 13×13 supercell, $E_e = -1$ eV, $m_e = 0.1m_0$, $E_b = 1.05$ eV, $m_b = 0.1248m_0$, $E_w = 0$ eV, $m_w = 0.0673m_0$. Plane waves are incident along the z direction.

ward the center, increasing symmetry and isolation from the electrodes. Likewise, in Fig. 6, where we plot transmission coefficient curves for impurities at different y locations and $x = z = 0$, the $n = 1$ transmission resonance is most strongly affected when $y = 0$, where the $n = 1$ cavity mode probability density maximum occurs. Thus a weakly attractive impurity has the greatest effect on the $n = 1$ resonance of a dot when placed in the center.

A strongly attractive impurity in a dot, on the other hand, gives rise to an $n = 1$ resonance mode typical of an impurity localized state and can be analyzed as an isolated impurity in a single barrier structure.²⁵ In Fig. 7, the $n = 1$ transmission resonance position, width, and maximum are plotted for a strongly attractive impurity ($\Delta U/t = -4.9$) at different locations along the z direction at $x = y = 0$. In this case, the resonance wave function is centered tightly around the impurity, and as the impurity is moved toward the center of the dot, the isolation from the electrodes (and hence the confinement of the impurity bound state) is increased and the resonance moves to higher energy. Note that this is opposite to the behavior in Fig. 5 where the $n = 1$ resonance has predominantly the nature of a cavity mode. The lateral location dependence of the $n = 1$ resonance position for a strongly attractive impurity, shown in Fig. 8, is also the

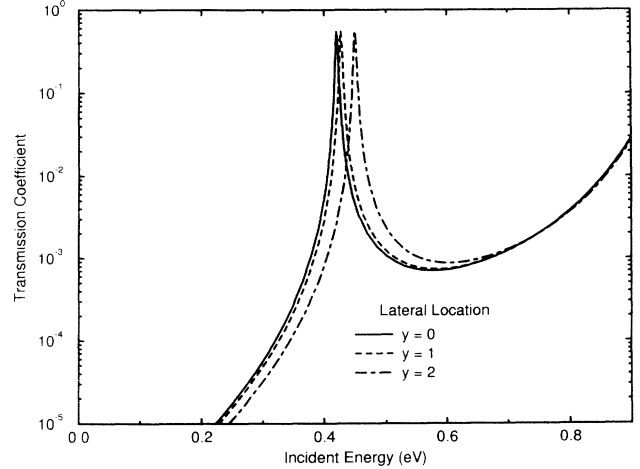


FIG. 6. Transmission coefficient curves for a rough-walled dot with a weakly attractive impurity ($\Delta U/t \approx -3.1$) in different lateral locations at $x = z = 0$. The rough-walled dot is that of sample 1 in Fig. 2. $a = 0.5$ nm, 13×13 supercell, $E_e = -1$ eV, $m_e = 0.1m_0$, $E_b = 1.05$ eV, $m_b = 0.1248m_0$, $E_w = 0$ eV, and $m_w = 0.0673m_0$. Plane waves are incident along the z direction.

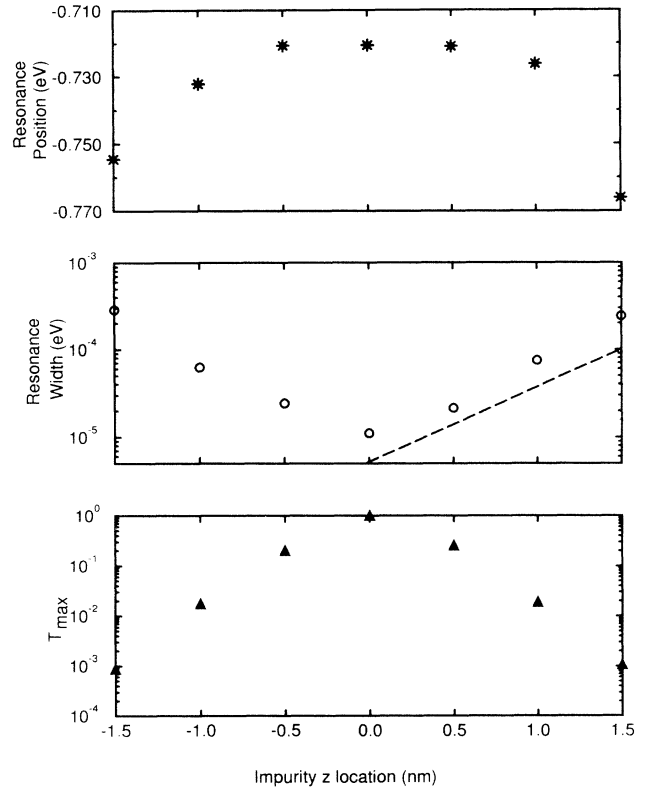


FIG. 7. Characteristics of the $n = 1$ transmission resonance for a rough-walled dot with a strongly attractive impurity ($\Delta U/t \approx -4.9$) in different z locations at $x = y = 0$. The rough-walled dot is that of sample 1 in Fig. 2. $a = 0.5$ nm, 13×13 supercell, $E_e = -1$ eV, $m_e = 0.1m_0$, $E_b = 1.05$ eV, $m_b = 0.1248m_0$, $E_w = 0$ eV, and $m_w = 0.0673m_0$. Plane waves are incident along the z direction. The dashed line in the middle panel indicates the rate at which the wave function magnitude decreases with distance from an attractive impurity.

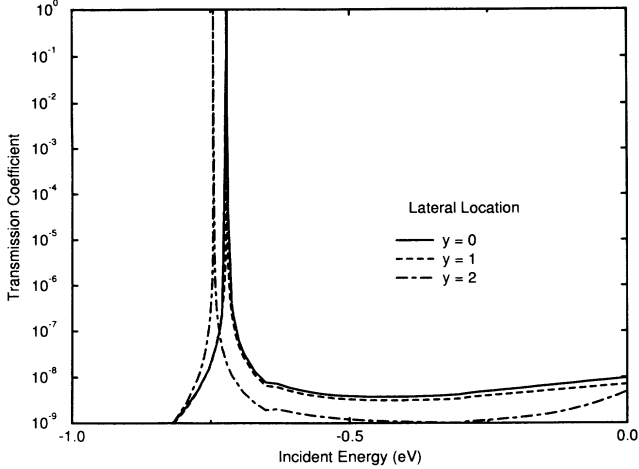


FIG. 8. Transmission coefficient curves for a rough-walled dot with a strongly attractive impurity ($\Delta U/t \approx -4.9$) in different lateral locations at $x = z = 0$. The rough-walled dot is that of sample 1 in Fig. 2. $a = 0.5$ nm, 13×13 supercell, $E_e = -1$ eV, $m_e = 0.1m_0$, $E_b = 1.05$ eV, $m_b = 0.1248m_0$, $E_w = 0$ eV, and $m_w = 0.0673m_0$. Plane waves are incident along the z direction.

opposite of that for weakly attractive impurities, as the impurity is moved toward the center, the confinement of the impurity level increases, raising the $n = 1$ resonance.

The dependence of the resonance width and maximum transmission coefficient on the impurity location along the z direction in the case of a strongly attractive impurity is also different from that in Fig. 5. Although the trends are the same (the resonance narrows and the maximum transmission coefficient increases as the impurity is moved toward the center), the effect is much greater in the case of a strongly attractive impurity (Fig. 7). The probability density of the impurity bound state drops off exponentially with distance from the impurity site, leading to the exponential dependence of resonance width and maximum transmission on impurity location. In the middle panel of Fig. 7, the dashed line shows the rate of decay of the resonant wave function: $|\psi|^2 \approx e^{-2\kappa d}$, where d is the distance from the impurity site and $\kappa = \cosh^{-1}(1 - E_1/2t)/a$. As the impurity is moved toward the center of the dot, interaction with the electrodes decreases exponentially, leading to an exponential decrease in the resonance width. The maximum transmission coefficient also increases as the impurity is moved toward the center of the dot, increas-

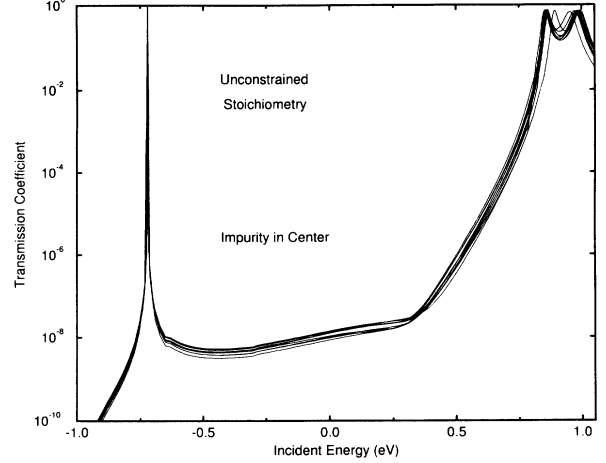


FIG. 9. The same as Fig. 2, except that a strongly attractive impurity ($\Delta U/t \approx -4.9$) is used.

ing symmetry along the z direction. This is analogous to the behavior in asymmetric double barrier structures: the maximum transmission coefficient increases exponentially as the well is moved toward the center of the structure and the barriers become equal in thickness. Note that the product of the resonance width and the maximum transmission increases as the impurity is moved toward the center in the case of a strongly attractive impurity, whereas the product is approximately constant for weakly attractive impurities. If we take this product as a measure of resonance strength, we see that a strongly attractive impurity near the center of the dot produces a stronger resonance than one near the edges.

An important observation in the case of strongly attractive impurities is that the $n = 1$ resonance position is nearly constant as long as the impurity is within a lattice constant or two of the center of the dot. The variation of resonance position over this range is less than that in the fluctuations of Fig. 2. This suggests there may be some hope of reducing fluctuations in resonance position due to interface roughness if a strongly attractive impurity can be placed near the center of a quantum dot. Indeed, only 1.4% of the electron probability density associated with the $n = 1$ mode of a dot with an impurity at $x = y = z = 0$ with $\Delta U/t = -4.9$ lies in the shell of interface roughness as opposed to 27.2% in the case of Fig. 2. Thus the $n = 1$ mode of a dot with an attractive impurity should sample the interface roughness less than without the impurity, leading to less fluctuation.

TABLE I. Standard deviations (σ_w) of the resonance widths of various sets of rough-walled dots expressed as a percentage of the difference between the resonance widths of the two corresponding reference structures without rough walls.

Impurity	Roughness stoichiometry	σ_w
none	unconstrained	11%
none	constrained	5%
$\Delta U/t = -3.97$	unconstrained	4.9%
$\Delta U/t = -4.9$	unconstrained	4.4%

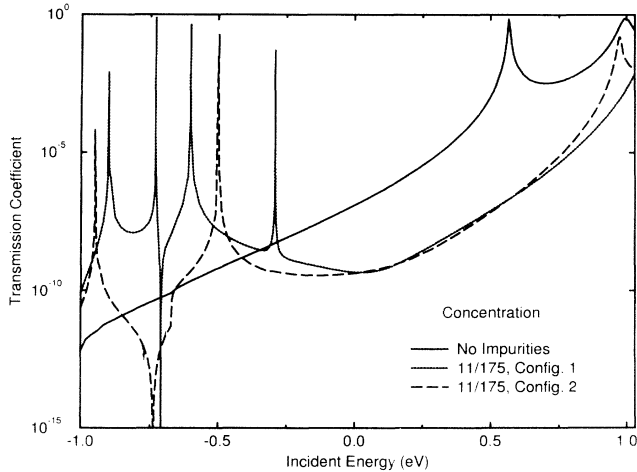


FIG. 10. Transmission coefficient curves for a rough-walled quantum dot with a concentration of $0.063/a^3$ strongly attractive ($\Delta U/t \approx -4.9$) impurities in the cavity (11 impurity sites were chosen at random out of the 175 sites within the cavity). Also shown is the transmission coefficient curve for the rough-walled dot of sample 1 in Fig. 2 (containing no impurities). $a = 0.5$ nm, 13×13 supercell, $E_e = -1$ eV, $m_e = 0.1m_0$, $E_b = 1.05$ eV, $m_b = 0.1248m_0$, $E_w = 0$ eV, and $m_w = 0.0673m_0$. Plane waves are incident along the z direction.

To analyze fluctuations in a dot with an impurity, we plot, in Fig. 9, transmission coefficient curves for the same set of ten dots as in Fig. 2, but with an impurity of strength $\Delta U/t = -4.9$ at $x = y = z = 0$. A glance at the figure reveals that the $n = 1$ resonance fluctuates over a much narrower energy range, as expected. Here the standard deviation of the $n = 1$ resonance position for the ten samples is 0.0007 eV compared with 0.008 eV without the impurity. The resonance width also fluctuates less; the standard deviation of the resonance widths is 4.4% of the difference between the widths of the two corresponding reference structures (the structures of Fig. 2 each with an impurity of strength $\Delta U/t = -4.9$ in the center).

Although a strongly attractive impurity has maximal effect, even a moderately attractive impurity can reduce fluctuations due to interface roughness. We have also calculated results for an impurity with $\Delta U/t = -3.97$, where about 9.1% of the probability density at the $n = 1$ resonance lies in the shell. Here we are in the cavity mode regime and the $n = 1$ resonance is above the well band edge. The standard deviation of the widths is 4.9% of the difference between the widths of the two corresponding

reference structures (the structures of Fig. 2 each with an impurity of strength $\Delta U/t = -3.97$ in the center). Results for the fluctuations of resonance width are summarized in Table I.

Thus an attractive impurity near the center of a quantum dot can reduce fluctuations due to variation in surface roughness. In a set of quantum dots with a single impurity very close to the center, the transmission characteristics are more uniform than without an impurity. If the impurity location is not controlled precisely, however, or if multiple impurities are present, fluctuations will still pose a problem. In fact, different impurity configurations at the same concentration can lead to completely different transmission spectra. To demonstrate this, we plot, in Fig. 10, transmission coefficient curves for the rough-walled dot of sample 1 in Fig. 9 with two different configurations of impurities in the cavity. Each configuration consists of 11 impurity sites placed at random among the 175 sites in the quantum dot. Also plotted in the figure is the transmission coefficient curve for the same rough-walled dot without impurities. We see that the high concentration of impurities produces a complex resonance structure, whose peak positions, widths, and maxima depend on the configuration.

IV. CONCLUSION

We have examined the effects of atomic-scale imperfections on the transmission properties of a quantum dot using a three-dimensional model of quantum transport. We have seen that sample to sample variations in interface roughness in a quantum dot could lead to fluctuations in the $n = 1$ transmission resonance position and width. We have also studied the effects of neutral impurities in quantum dots as a function of impurity strength and location and seen that an attractive impurity near the center of the dot draws in the $n = 1$ resonance wave function away from the rough interface and thereby reduces fluctuations. Nonetheless, the presence of more than a single impurity in a dot can lead to complex, impurity configuration dependent resonance structure, especially at high concentrations.

ACKNOWLEDGMENTS

The authors would like to thank Dr. Eric F. Van de Velde for helpful discussion. S.K.K. would like to thank the Office of Naval Research for support during this work. This work was also supported by the Office of Naval Research under Grant No. N00014-89-J-1141.

¹ W. Chu, C. C. Eugster, and A. Moel, *J. Vac. Sci. Technol. B* **10**, 2966 (1992).

² K. Yoh, K. Kyomi, and A. Nishida, *Jpn. J. Appl. Phys. Pt. 1* **31**, 4515 (1992).

³ Y. Qian, J. M. Zhang, and J. Y. Xu, *Superlatt. Microstruct.* **13**, 241 (1993).

⁴ K. Inoue, K. Kimura, and K. Maehashi, *J. Cryst. Growth* **127**, 1041 (1993).

- ⁵ X. Q. Shen, M. Tanaka, and T. Nishinaga, *J. Cryst. Growth* **127**, 932 (1993).
- ⁶ S. Tsukamoto, Y. Nagamune, and M. Nishioka, *Appl. Phys. Lett.* **62**, 49 (1993).
- ⁷ H. Iwano, S. Zaima, Y. Koide, and Y. Yasuda, *J. Vac. Sci. Technol. B* **11**, 61 (1993).
- ⁸ K. Kash, B. P. Van der Gaag, D. D. Mahoney, A. S. Gozdz, L. T. Florez, J. P. Harbison, and M. D. Sturge, *Phys. Rev. Lett.* **67**, 1326 (1991); *Nanostructure Physics and Fabrication*, edited by M. A. Reed and W. P. Kirk (Academic, San Diego, 1989).
- ⁹ T. Itoh, S. Nobuyuki, and A. Yoshii, *Phys. Rev. B* **45**, 14 131 (1992).
- ¹⁰ V. V. Mitin, *Superlatt. Microstruct.* **8**, 413 (1990).
- ¹¹ P. L. Mceuen, B. W. Alphenaar, and R. G. Wheeler, *Surf. Sci.* **229**, 312 (1990).
- ¹² C. C. Eugster, J. A. del Alamo, M. R. Melloch, and M. J. Rooks, *Phys. Rev. B* **46**, 10 146 (1992).
- ¹³ E. Tekman and S. Ciraci, *Phys. Rev. B* **42**, 9098 (1990).
- ¹⁴ P. F. Bagwell, *Phys. Rev. B* **41**, 10 354 (1990); A. Kumar and P. F. Bagwell, *ibid.* **43**, 9012 (1991); P. F. Bagwell, T. P. Orlando, and A. Kumar, in *Resonant Tunneling in Semiconductors*, edited by L. L. Chang *et al.* (Plenum Press, New York, 1991), p. 417.
- ¹⁵ C. S. Chu and R. S. Sorbello, *Phys. Rev. B* **40**, 5941 (1989).
- ¹⁶ Y. Takagaki and D. K. Ferry, *Phys. Rev. B* **45**, 6715 (1992).
- ¹⁷ D. van der Marel and E. G. Haanappel, *Phys. Rev. B* **39**, 7811 (1989); E. G. Haanappel and D. van der Marel, *ibid.* **39**, 5484 (1989).
- ¹⁸ J. A. Nixon, J. H. Davies, and H. U. Baranger, *Phys. Rev. B* **43**, 12 638 (1991).
- ¹⁹ W. R. Frensley, *Rev. Mod. Phys.* **62**, 745 (1990).
- ²⁰ C. S. Lent and D. J. Kirkner, *J. Appl. Phys.* **67**, 6353 (1990).
- ²¹ W. R. Frensley (private communication).
- ²² D. Z.-Y. Ting, E. T. Yu, and T. C. McGill, *Phys. Rev. B* **45**, 3583 (1992).
- ²³ Roland W. Freund and Noel M. Nachtigal, *Numer. Math.* **60**, 315 (1991).
- ²⁴ E. F. Van de Velde, *Concurrent Scientific Computing* (Springer-Verlag, New York, 1994).
- ²⁵ S. K. Kirby, D. Z.-Y. Ting, and T. C. McGill, *Phys. Rev. B* **48**, 15 237 (1993).